

# Flow Field Analysis of Intelligent Downhole Flow Control Valve

Chuan Li, Dongsheng He, Yiwei Yang, Xiaolu Xie, Hui Dai and Bo Wang

School of Mechatronic Engineering, Southwest Petroleum of University, Chengdu, Sichuan 610500, China.

---

## Abstract

Through the establishment of the flow model of the intelligent well flow control valve in the first production layer downhole, The numerical simulation and theoretical analysis of the flow control valve were carried out under different openings and different pressure differences, Furthermore, the distribution of internal flow field is analyzed, and it is obtained that the speed and flow rate of internal flow field are consistent with the results obtained by theoretical analysis. It is found that the velocity at the orifice at the three openings decreases with the increase of the opening and increases with the increase of the pressure difference. Among them, at the maximum pressure difference of 0.5 MPa, the opening orifice velocity The maximum speed is 37.79 m/s and the speed at the orifice is fast, which will cause erosion of the flow control valve structure. As the opening degree increases, the average outlet flow also increases, When the opening is unchanged, the average flow rate at the outlet increases as the pressure difference increases within the range of 0.1 MPa to 0.5 MPa. It was found that when the maximum pressure difference was 0.5 MPa, the output of opening degree one and opening degree two reached 12.07% and 47.78% of the total output of opening degree three, respectively. When the maximum pressure difference and maximum opening degree reached 7024.32 m<sup>3</sup>/d. In summary, the analysis of the flow field of the flow control valve provides a reference value for structural optimization, erosion research and production improvement.

## Keywords

Intelligent well; Flow control valve; Flow rate; Flow field analysis; Numerical simulation.

---

## 1. Introduction

Intelligent well technology is one of the major breakthroughs in oilfield production technology in recent years[1], It is widely used to improve production performance, realize real-time control and production optimization, and maximize the ultimate oil recovery [2].The intelligent well is mainly composed of downhole flow control valve (ICV), downhole pressure gauge and multi-port straight-through packer [3]. The flow control valve is one of the core components of fluid control systems in different production layers. Its working principle is to realize downhole flow control by changing the throttling area of the throttling hole.

Intelligent well flow control valves research abroad, HS - ICV series flow control valve is mainly included two types, the first kind of flow control valve orifice for circular orifice [4], only full open and close the opening of two gear flow control, after the upgrade of the second generation has increased among throttling state, intermediate state of the throttle opening adjustment can be accomplished, and the flow channel and the metal seal use the tungsten carbide coating on the surface, improve the ability to resist wear and erosion resistance of flow control valve. IV-ICV series flow control valves adopt stepless regulation throttling hole, which can realize stepless regulation of valve opening flow [5]. Hcm-a is A multi-gear regulating flow control valve, which realizes multi-position

regulating throttling downhole. In addition to the two states of opening and closing, the standard J-shaped casing design also provides multiple throttling gear with the total area of external throttling of 3%, 6%, 9%, 12%, 15% and 20% [6]. At present, the research on downhole flow control valve of intelligent well is still in its infancy in China, and the design of flow control valve throttling hole still lacks the corresponding theoretical basis. Most designs mainly rely on experience and test, and the design cycle is long and the cost is high.

This paper will take the flow control valve as the research object to analyze the flow field of the flow control valve and verify it through theoretical analysis, providing a reference for the optimization of the flow control valve structure.

## 2. Flow Control Valve Structure and Principle

In order to obtain the calculation model of flow control valve output, the structure and working principle of flow control valve [7][8] need to be analyzed first. By simplified model of the production in layer flow control valve flow and to establish the flow control valve of the three-dimensional structure as shown in Fig. 2-1, its working principle: when the stroke cylinder left open, after a steady flow hole opened the first opening, crude oil through the annulus between casing and flow control valve shell inflows, and then through the orifice into the cylinder, out in the end. The same goes for the second and third.

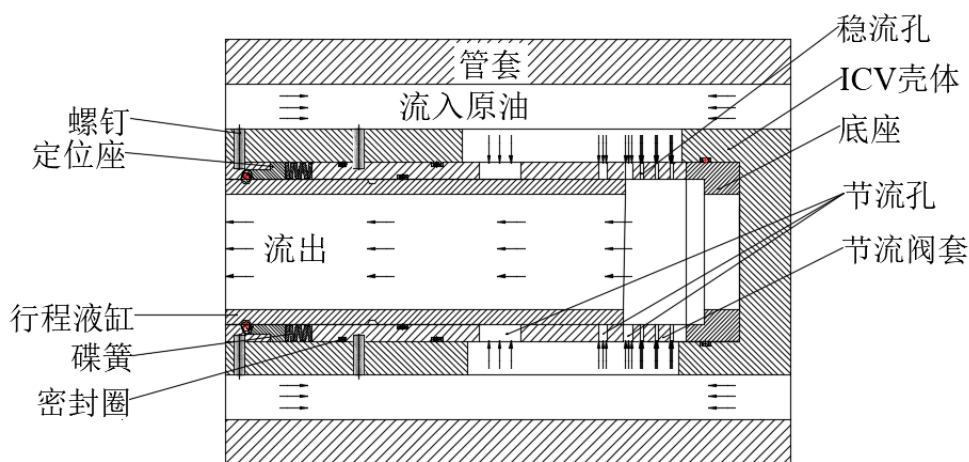


Fig. 2-1 Flow model of flow control valve

## 3. Flow Field Analysis of Flow Control Valve

### 3.1 Geometry processing

In order to better reflect the flow situation of the flow field and considering the computer performance, the model is appropriately simplified in modeling. SolidWorks is used to build three models with open degree respectively, and then the runner is extracted from ANSYS Spaceclaim respectively. Fig. 2-2 shows the runner with open degree 1:

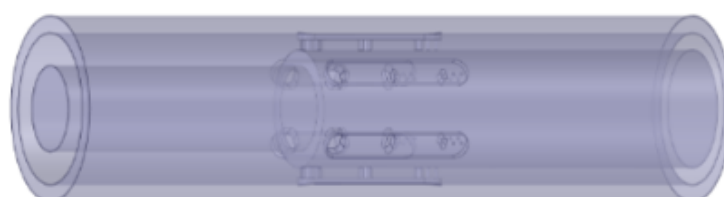


Fig. 2-2 The model after extracting the runner

### 3.2 Meshing

Poly - Hexcore mesh was divided by Fluent Meshing as shown in Fig. 3-2.

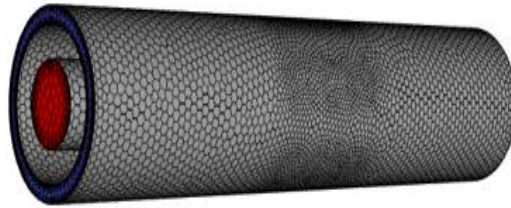


Fig. 3-2 Meshing

### 3.3 Parameter Settings

#### 3.3.1 Create the crude oil material

The fluid medium used for flow field numerical simulation of flow control valve is crude oil. The depth of the oil reservoir is 2195 m, the density of crude oil is  $0.811 \text{ g/cm}^3$ , the dynamic viscosity of crude oil is  $2.14 \text{ MPa}\cdot\text{s}$ , the temperature of the oil reservoir is  $70^\circ\text{C}$ , the specific heat capacity of crude oil is  $2310 \text{ J}/(\text{kg}\cdot^\circ\text{C})$ , and the thermal conductivity is  $0.14 \text{ W}/(\text{M}\cdot^\circ\text{C})$  and the thermal expansion coefficient of crude oil is  $880 \times 10^{-6}/\text{K}$  [9].

#### 3.3.2 Watershed and boundary conditions setting

Materials were selected to create a turbulence model for crude oil that was selected as a standard  $K - \epsilon$  model. inlet adopts a pressure inlet, inlet pressure is selected to be  $20 \text{ MPa}$ . For Outlet setting, in order to avoid boundary backflow, the Outlet boundary is set as an open Outlet boundary, and the pressure difference between the open Outlet boundary and the inlet boundary is set as  $0.1 \sim 0.5 \text{ MPa}$ . The default boundary without sliding wall is selected for the wall boundary condition.

## 4. Simulation Results and Analysis

In this paper, models were built and flow field numerical simulation was carried out under 15 conditions of opening I, opening II and opening III at  $0.1 \text{ MPa}$ ,  $0.2 \text{ MPa}$ ,  $0.3 \text{ MPa}$ ,  $0.4 \text{ MPa}$  and  $0.5 \text{ MPa}$  respectively [10]. Here, velocity cloud charts of opening I, Opening II and opening III at  $0.5 \text{ MPa}$  were presented as examples.

### 4.1 Simulation Results

#### 4.1.1 Opening I simulation results

When the pressure difference is  $0.1 \text{ MPa} \sim 0.5 \text{ MPa}$ , the data of average flow rate, maximum flow rate and outlet flow rate of the flow control valve are extracted from the opening I. The calculation results of flow rate and pressure difference of the throttle hole are shown in Table 4-1 and the velocity cloud figure is shown in Fig. 4-1.

Table 4-1 The solution result of opening I under different pressure difference

Different pressure difference MPa	Average outlet flow $\text{m}^3/\text{d}$	Mean flow rate of orifice ( $\text{m}/\text{s}$ )	Average outlet velocity ( $\text{m}/\text{s}$ )
0.1	432	16.6	1.15
0.2	604.8	23.66	1.65
0.3	777.6	28.86	2.03
0.4	881.28	33.54	2.23
0.5	984.96	37.79	2.71

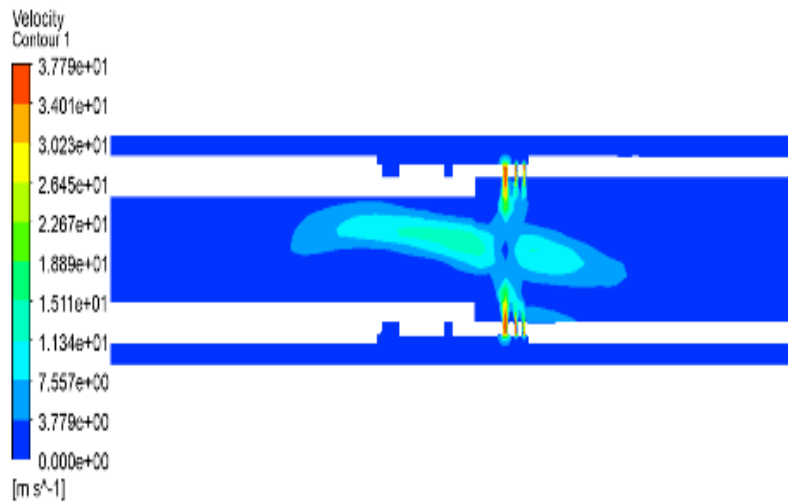


Fig. 4-1 Opening I speed cloud

4.1.2 Open II simulation results

When the pressure difference is 0.1 MPa ~ 0.5 MPa, the data of average flow rate, maximum flow rate and outlet flow rate of the flow control valve are extracted from the opening II. The calculation results of flow rate and pressure difference of the throttle hole are shown in Table 4-2 and the velocity cloud figure is shown in Fig. 4-2.

Table 4-2 The solution result of opening II under different pressure difference

Different pressure difference MPa	Average outlet flow $m^3/d$	Mean flow rate of orifice (m/s)	Average outlet velocity (m/s)
0.1	1555.2	16.23	3.83
0.2	2160	23.18	5.45
0.3	2678.4	28.43	6.70
0.4	3024	32.75	7.81
0.5	3456	36.79	8.61

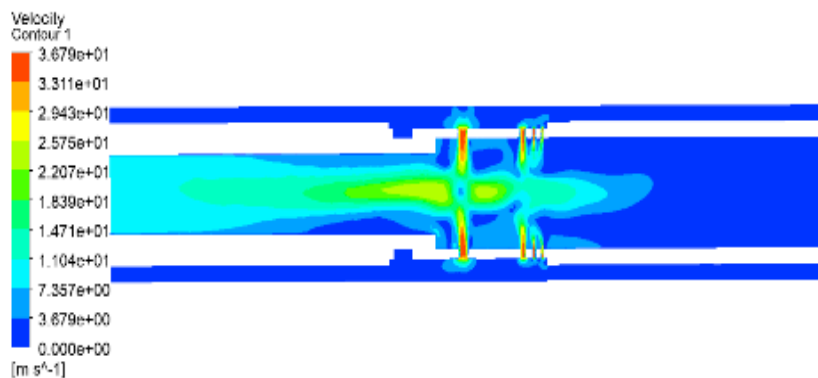


Fig. 4-2 Opening II speed cloud

4.1.3 Open III simulation results

When the pressure difference is 0.1 MPa ~ 0.5 MPa a, the data of average flow rate, maximum flow rate and outlet flow rate of the flow control valve are extracted from the opening III. The calculation results of flow rate and pressure difference of the throttle hole are shown in Table 4-3 and the velocity cloud figure is shown in Fig. 4-3.

Table 4-3 The solution result of opening III under different pressure difference

Different pressure difference MPa	Average outlet flow $m^3/d$	Mean flow rate of orifice ( $m/s$ )	Average outlet velocity ( $m/s$ )
0.1	3110.41	13.47	7.46
0.2	4380.48	19.07	10.58
0.3	5356.82	23.43	12.96
0.4	6220.82	27.01	14.97
0.5	7024.32	30.19	17.75

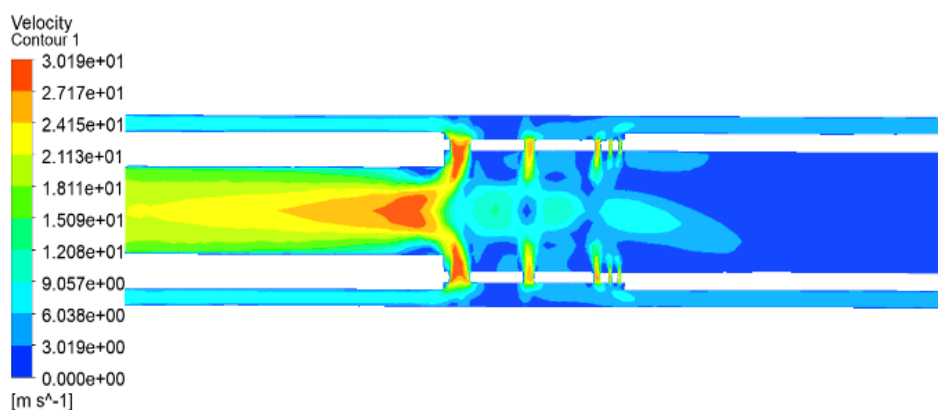


Fig. 4-3 Opening III speed cloud

### 4.2 Analysis of results

The average outlet flow results of the first, second and third opening when the pressure difference is 0.1 MPa ~ 0.5 MPa are statistically calculated, as shown in Fig. 4-4.

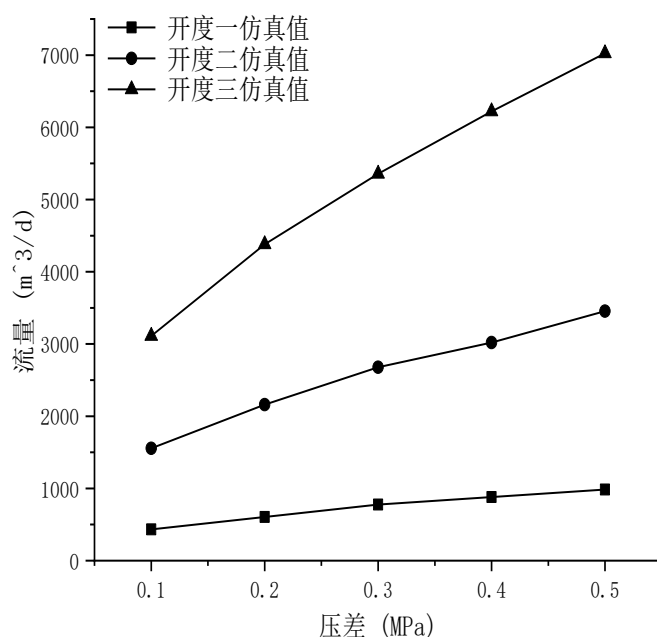


Fig . 4-3 Simulation flow rate when pressure difference is 0.1MPa ~ 0.5 Mpa

As shown in Table 4-1~4-3, when the maximum pressure difference is 0.5 MPa, the maximum flow amount of open I, open II and open III is  $984.96\text{ m}^3/\text{d}$ ,  $3456\text{ m}^3/\text{d}$  and  $7024.32\text{ m}^3/\text{d}$ , respectively. As shown in Fig. 4-3, the flow rate increases with the increase of opening and pressure difference. As shown in Fig.4-1 ~ Fig. 4-3, the maximum velocity appears in the flow field area in the throttle hole of the flow control valve. The maximum velocity of open I, open II, open III is  $37.79\text{ m/s}$ ,  $36.79\text{ m/s}$ ,  $30.19\text{ m/s}$ , and the average velocity at the exit of the flow control valve is  $2.7\text{ m/s}$ ,  $8.61\text{ m/s}$ , and  $17.75\text{ m/s}$ . The speed at the three orifice openings is very high, which will cause erosion to the orifice, which provides an important reference for optimizing the flow control valve structure and reducing erosion.

### 5. Theoretical Analysis

As a comparison, this paper conducts a theoretical analysis of the flow rate of the flow control valve. According to the flow formula 4-1, the outlet flow rates of the three opening of open I, open II and open III under the maximum pressure difference of 0.1 Mpa ~0.5 MPa are obtained:

$$q = C_d A \sqrt{\frac{2\Delta P}{\rho}} \tag{5-1}$$

In the above formula:

$C_d$  discharge coefficient

$A$  Orifice area

$\Delta P$  Different pressure difference

$\rho$  density

When open I  $l/d=0.8$ , the flow coefficient is 0.8; when open II and open III,  $l/d=0.45$ , the flow coefficient is 0.6[11]. Each parameter is substituted into formula 5-1 to obtain the comparison between the theoretical results and the simulation results of flow Q, as shown in Fig . 5-2.

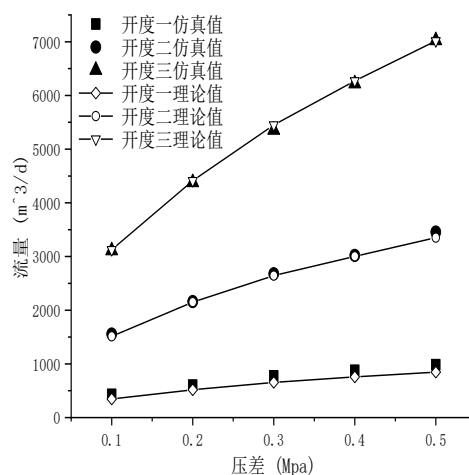


Fig. 5-2 Simulation results and theoretical results

In order to express the theoretical results and the simulation results more intuitively, it can be seen from Figure 5-2 that the flow rates of open I, open II and open III .all increase with the increase of pressure difference, and also increase with the increase of opening. Compared with the simulation results shown in Figure 4-3, the theoretical analysis results differ little from the simulation results.

## 6. Conclusion

In this paper, through numerical simulation, and draw the flow control valve flow and pressure difference curve. Compared with the theoretical analysis results, the results show that the simulation results is in good agreement with the theoretical results. The following conclusions can be drawn:

- (1) A simulation cloud image reveals that the maximum velocity of the three openings is  $37.7m/s$  at the orifice. A maximum velocity of  $37.79m/s$  at the opening is suggested as erosion due to excessive speed. This provides a reference for erosion and structural optimization of flow control valves.
- (2) By comparison, it can be seen that the simulation solution is basically the same as the theoretical solution, and the curve does not completely coincide, because the theory takes a fixed value, while the actual flow rate in the simulation changes continuously with the increase of the opening, and the pressure difference between the inlet and outlet does not take into account the pressure loss of the flow passage. The results can be used as reference data.
- (3) Under the same opening, the average flow rate increases with the increase of pressure difference. At the same time, when the pressure difference is constant, the average outlet flow rate increases with the increase of opening rate. The speed at the throttle orifice decreases with the increase of the opening.
- (4) It was calculated that the output under the maximum pressure difference of the first and second opening reached 12.07% and 47.78% of the total output respectively. When the third opening of the flow control valve is opened, its flow is  $7015.68m^3/d$ .

The numerical simulation not only provides data reference for the study of erosion at the throttling hole, but also provides reference for the optimal design of flow control valve.

## References

- [1] ILAMAHO, WATERHOUSER. FIELD-SCALE Production Optimization with Intelligent Wells [C]. SPE Europec featured at 80th EAGE Conference and Exhibition, 2018.
- [2] WANG J, ZHANG N, WANG Y, et al. Development of a downhole incharge inflow control valve in intelligent wells[J]. Journal of Natural Gas Science and Engineering, 2016, 29: 559-569.
- [3] KAMAL S M M, TERAN J M P, M ADAMAWIM, et al. Retrieval of Intelligent Completions Challenges and Solution [C]. SPE/IADC Middle East Drilling Technology Conference and Exhibition, 2018.
- [4] Jeses Constantine. Installation and Application of an Intelligent Nigeria[R]. SPE116133, 2004.
- [5] Jifeng Yang, Yongrui Zhao et al. Technology and application of intelligent completion flow control equipment [J]. Oil field machinery. 2013 42(3): 66-70.
- [6] Jameel U. Rahman, Clifford Allen, Gireesh Bhat. Second-Generation Interval Control Valve (ICV) Improves Operational Efficiency and Inflow Performance in Intelligent Completions[J]. North Africa Technical Conference and Exhibition Cairo, Egypt 2012.
- [7] Jie Qian, Zejun Shen. et al. Opportunities and Challenges of intelligent completion technology development in China, Petroleum Geology and Engineering, 2009, 23(2):76-79.
- [8] Dong Guo. Parametric design and Analysis of downhole flow controller of intelligent Well [D]. Southwest Petroleum University 2018: 10-60.
- [9] Kang Zhao. Integrated design and Analysis of downhole flow controller of intelligent well [D]. Southwest Petroleum University, 2017:55-73.
- [10] Aini Maimaitimgin ANSYS Workbench 18.0 Introduction and Application of finite element Analysis [M]. Beijing: Machinery Industry Press, 2018: 101-104.
- [11] Fuling Xu, Yaoming Chen. Hydraulic and pneumatic transmission [M]. Machinery Industry Press, 1997: 22-28.